ACS OMEGA

Article

Cite This: ACS Omega 2018, 3, 3830−3834

Cobalt-Based Coordination Polymer for Oxygen Reduction Reaction

Prabu Mani,[†] Anjaiah Sheelam,[‡,⊥] Shubhajit Das,[§,⊥] Guanxiong Wang,[∥] Vijay K. Ramani,[∥] Kothandaraman Ramanujam,[‡] Swapan K. Pati,[§] and Sukhendu Mandal*[,†]

[†]School of Chemistry, Indian Institute of Science Education and Research Thiruvananthapuram, Thiruvananthapuram, Kerala 695551, India

[‡]Department of Chemistry, Indian Institute of Technology Madras, Chennai 600036, India

[§]New Chemistry Unit and Theoretical Science Unit, Jawaharlal Nehru Centre for Advanced Scientific Research, Bangalore 560064, India

[∥]Department of Energy, Environmental and Chemical Engineering, Washington University in St. Louis, St. Louis, Missouri 63130, United States

Supporting Information

ABSTRACT: Lack of control over the structure and electrically nonconductive properties of coordination polymers (CPs) creates a major hindrance to designing an active electrocatalyst for oxygen reduction reaction (ORR). Here, we report a new semiconductive and low-optical band gap CP structure $[\{Co_3(\mu_3\text{-}OH)(BTB)_2(BPE)_2\}\{Co_{0.5}N(C_5H_5)\}]$, **1**, that exhibits high-performance ORR in alkaline medium. The electrical conductivity of compound **1** was measured using impedance spectroscopy and found to be 5×10^{-4} S cm^{-1}. The Ketjenblack EC-600JD carbon used as a support for all the electrochemical methods such as cyclic voltammetry, rotating disk electrode, rotating ring-disk electrode and Koutecký−Levich analysis. The as-synthesized Co-based catalyst has the ability to reduce O_2 to H_2O by a nearly four-electron process. The crystal structure of **1** shows that the trimeric unit $\{Co_3(\mu_3\text{-}OH)(COO)_5N_3\}$ and monomeric unit $\{Co(COO)_2(NC_5H_4)_2\}^{2+}$ are linked with BTB and BPE linkers to form a three-dimensional structure. Theoretical calculations predict that the monomeric center acts as an active catalytic site for ORR. This could be due to the efficient overlap of highest occupied molecular orbital−lowest unoccupied molecular orbital between monomer and O_2 molecule. This CP, **1**, shows facile 3.6-electron ORR, and it is inexpensive compared with widely used Pt catalysts. Therefore, this CP can be used as a promising cathode material for fuel cells in terms of efficiency and cost effectiveness.

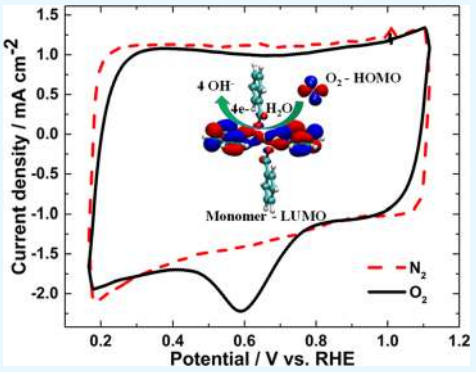

INTRODUCTION

Oxygen reduction reaction (ORR) is a fundamental reaction related to energy conversion.[1] It gains much interest in fuel cells or lithium−air batteries because of its essential role in them.[2] Optimization of an electrocatalyst is necessary either to enhance the efficiency of the fuel cell or to increase the kinetics rate of ORR.[3] Pt-based materials are most effective ORR catalysts, but there is a need to replace them for cost effectiveness.[3] It is quite difficult to synthesize an ideal catalyst for ORR because of several factors that will interfere with the desired architecture and electronic properties. Among several desirable characteristics, high active site density, stability in electrolyte/oxygen and peroxide, reusability, and low overpotential relative to the thermodynamic of 4e$^-$ oxygen-to-water reduction potential of 1.23 eV are very impotent for effective ORR catalysts. It has been shown that transition-metal-, nitrogen-, and carbon-containing compounds having an M−N_x structural motif can act as an effective ORR catalyst, where M is nonplatinum metal, and in most of the cases, it is Fe or Co or Cu or Ni, which is chelated with nitrogen atoms of the ligand.[4−6] The structure with an M−N_x motif exhibits good ORR activity but suffers difficulty in terms of stability in various electrolytes. Thermal treatment can get rid of this stability issue, but it introduced new challenges to find out catalytic active sites, which are essential for catalyst optimization and mechanistic understanding. Thus, there is a demand for chemically and electrochemically stable ORR electrocatalysts with well-defined catalytic sites.

A hierarchy of architectures, tunable chemical structure, and high surface area lead to tailor-made pores for controllable reactions and maximize active sites. These characteristics make metal−organic frameworks (MOFs) or coordination polymers (CPs) potential candidates for electrocatalysis. However, most of the MOFs or CPs are electrical insulators, which limit their use in electrocatalytic applications.[7−9] Recent synthetic modifications have given rise to conductive MOFs, and few of these exhibit electrocatalysis.[10,11] Recently, Miner et al. have used a conductive MOF, Ni_3(hexaiminotriphenylene)$_2$, as an

Received: January 16, 2018
Accepted: March 14, 2018
Published: April 4, 2018

DOI: 10.1021/acsomega.8b00088
ACS Omega 2018, 3, 3830−3834

ORR catalyst.[12] However, this conductive MOF reduces oxygen to H_2O_2 (87.5%) by a $2e^-$ process. Jahan et al. reported $4e^-$ transfer ORR pathways using a composite of graphene–metalloporphyrin MOFs.[13] Therefore, there is a high demand for synthesizing conductive or semiconductive MOFs or CPs for electrochemical applications.

It is to be noted that MOFs or CPs have been used as ORR catalysts either by making composites containing graphene oxide and porphyrin or by making porous carbonaceous materials using high-temperature pyrolysis.[13−18] Here, our aim is to design and synthesize a nonplatinum metal-based conductive MOF or CP by controlling the structure and chemical and electronic properties for targeted ORR catalysts. We introduce $[\{Co_3(\mu_3\text{-}OH)(BTB)_2(BPE)_2\}\{Co_{0.5}N(C_5H_5)\}]$, **1**, a new three-dimensional CP structure with an optical band gap energy of 1.83 eV, which facilitates ORR via a 3.6-electron reaction. This CP retains its current density during ORR and shows no morphological degradation due to electrochemical reactions. These characteristics make it one of the promising nonplatinum-group metal ORR catalysts.

RESULTS AND DISCUSSION

Compound **1** was synthesized solvothermally using $CoCl_2$ (0.25 mmol), 1,3,5-tris(4-carboxyphenyl)benzene (0.05 mmol) (BTB), 1,2-bis(4-pyridyl)ethane (0.1 mmol) (BPE), and DMF–H_2O solvent mixture on heating at 120 °C for 72 h (see the Supporting Information). Purple-colored needle-shaped crystals were characterized using single-crystal X-ray diffraction, powder X-ray diffraction (PXRD), thermogravimetric analysis (TGA), IR, and so forth. They have a three-dimensional structure, where $\{Co_3(\mu_3\text{-}OH)(COO)_5N_3\}$ and $\{Co(COO)_2(NC_5H_4)_2\}$ units are linked with BTB anions (Figure 1a).

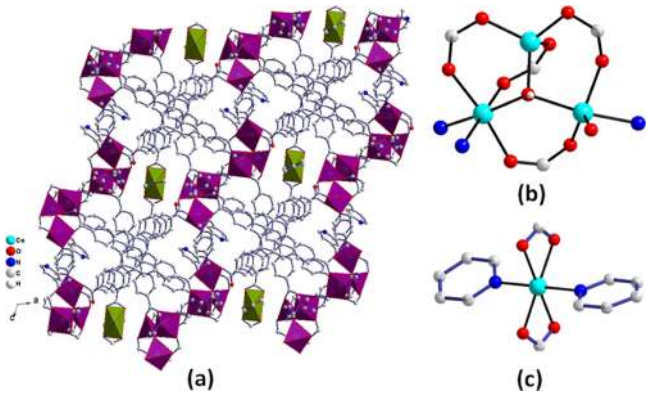

Figure 1. (a) Three-dimensional structure of compound **1** along the *ac* plane. (b,c) Trimer and monomer units, respectively, present in the compound.

The trimeric unit, $\{Co_3(\mu_3\text{-}OH)\ (COO)_5N_3\}$, is built from three different cobalt centers, where one is distorted tetrahedral $Co(1)O_4$, another is distorted trigonal bipyramid $Co(2)O_4N$, and the third one is distorted octahedral $Co(3)O_4N_2$ units (Figure 1b). The three Co^{II} ions are linked through a bridge OH group, forming a scalene triangle (with Co···Co distances in the range of 3.172–3.712 Å). In the monomer unit, $\{Co_{0.5}(COO)_2(NC_6H_5)\}$, the cobalt ion has a distorted octahedral geometry with two carboxylate moieties and two pyridine molecules (Figure 1c). The formation of a pyridine molecule is in situ, and it could be formed from a BPE molecule. The connectivity of the cobalt trimer and monomer with BPE and BTB ligands forms the three-dimensional structure. Topological analysis showed a structure topological network with 6, 12, 13, 14-c net with stoichiometry (6-c)(12-c)2(13-c)2(14-c)2; 4-nodal net.[19]

PXRD data of the as-synthesized compound **1** match with the simulated PXRD pattern, indicating the phase purity of the compound (Figure S1a). Thermogravimetric data show that compound **1** is stable up to 300 °C (Figure S2). The IR spectrum exhibits the characteristic peaks of organic struts (Figure S3). The optical band gap energy was calculated from the diffuse reflectance spectra, and it was found to be 1.83 eV (Figure S4). N_2 adsorption isotherm confirms the nonporous nature of the compound (Figure S5). We have measured the impedance for compound **1** (without conducting carbon) by making a pellet with a 0.25 mm thickness and a 1.0 cm^2 area. Impedance spectroscopy was performed at open-circuit potentials with a frequency range of 100–1 kHz (Figure 2).

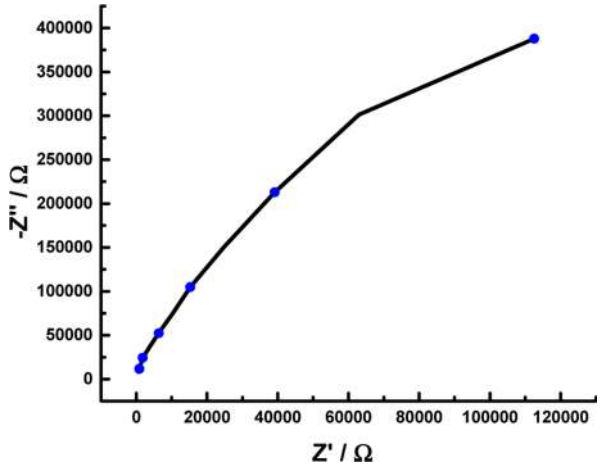

Figure 2. Impedance graph for compound **1**.

The conductivity of the compound **1** is 5×10^{-4} S cm^{-1}, calculated using eq 1. The conductivity value of the compound **1** suggests that it is a semiconductor.

$$\sigma = \frac{l}{Ra} \tag{1}$$

where σ stands for the conductivity, R stands for the resistance, l stands for the thickness of the material, and a stands for the area of the material.

The semiconductive nature and stability of compound **1** in KOH solution provoked us to explore its electrochemical characteristics (Figures S4 and S1b). The cyclic voltammogram of compound **1** (recorded with 20 mV s^{-1} at room temperature) on glassy carbon rotating disk electrodes exhibits a featureless voltammetric current in a N_2 atmosphere. Under an O_2 atmosphere, it clearly exhibits a well-defined reduction peak current with an onset potential of 0.81 V versus RHE in 0.10 M solution of KOH (Figure 3). This proved that compound **1** can enhance the ORR activity of the glassy carbon electrode.

To assess the suitability of compound **1** as an electrocatalyst for cathode ORR, we have investigated the methanol tolerance ability of the catalyst in oxygen-saturated 0.1 M KOH containing 1 M methanol (Figure S6). The measurements show that no influence was detected due to the presence of

DOI: 10.1021/acsomega.8b00088
ACS Omega 2018, 3, 3830−3834

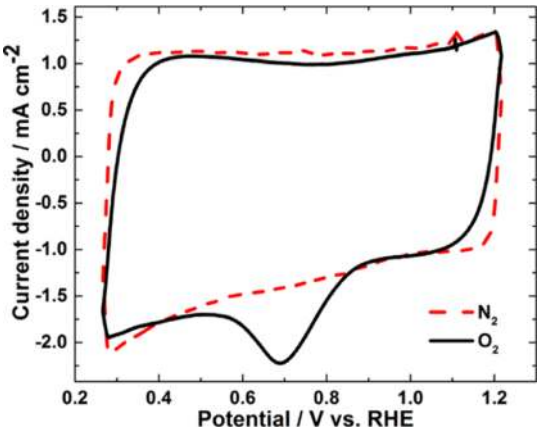

Figure 3. Cyclic voltammogram of compound **1** in 0.1 M KOH electrolyte saturated with O_2 and N_2 at room temperature.

methanol. This confirms the methanol tolerance of the catalyst, and we can conclude that compound **1** can be used as a cathode for the direct methanol fuel cell (DMFC).

The kinetics studied through rotating disk voltammetry provide in-depth information toward the electron-transfer kinetics of compound **1** during ORR. The voltammetric profiles show that, with the increase of rotation speed of the electrode, the current density is enhanced (Figure S7). Koutecky–Levich (K–L) plots measured at various potentials in the ORR regime are nearly parallel to the theoretical four-electron line, indicating the near complete reduction of oxygen into OH^- ions. Moreover, the linearity of the plots suggests the first-order reaction kinetics for ORR (Figure 4).

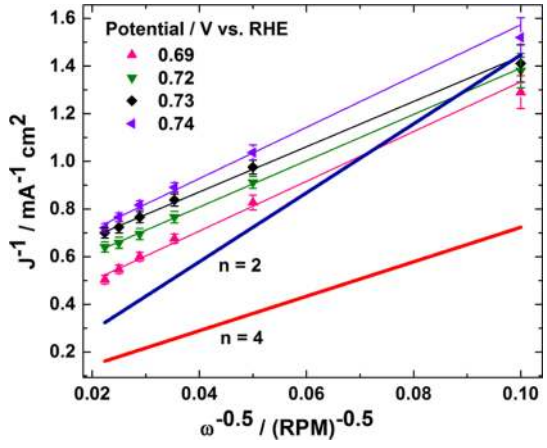

Figure 4. K–L plots of compound **1** studied at different electrode potentials.

Rotating ring-disk electrode (RRDE) analysis was performed by coating the disk portion of the RRDE with the compound **1**. In addition, the ring was posted at 0.45 V versus RHE to detect the intermediates of ORR generated out of the disk (Figure S8). Using the following eqs 2 and 3, we have calculated the number of electrons (n) and % of hydrogen peroxide (H_2O_2) liberated during the ORR. If the O_2 undergoes complete reduction into OH^-, n would be 4 and hydrogen peroxide production would be 0%. The intermediates generated at the disk, such as peroxide, can oxidize at the ring as it is biased at 0.45 V versus RHE. From the obtained I_{disk} and I_{ring} values of the RDE experiment, n values were calculated and it was in between 3.4 and 3.6 in the potential range of 0.85–0.40 V versus RHE (Figure 5), implying that ORR proceeds through

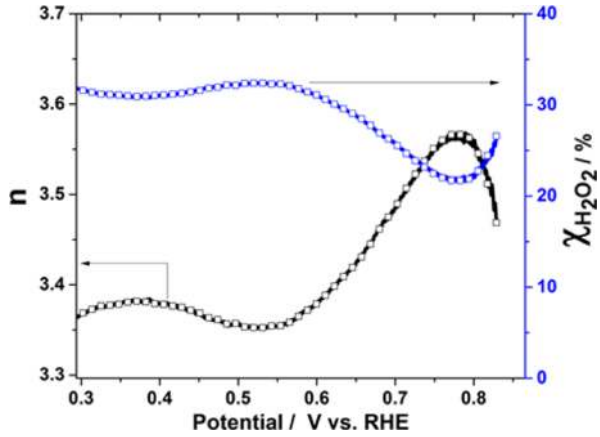

Figure 5. Number of electrons and percentage of hydrogen peroxide production during the ORR using compound **1**.

nearly four-electron-transfer pathway with compound **1**. The H_2O_2 production rate was 20–30% in the ORR region.

$$n = \frac{4I_{disk}}{I_{disk} + I_{ring}/\text{C. E}} \quad (2)$$

$$\chi_{H_2O_2} = \frac{200 \times I_{ring}/\text{C. E}}{I_{disk} + I_{ring}/\text{C. E}} \quad (3)$$

where I_{ring}, I_{disk}, and C.E stand for the ring current, disk current, and collection efficiency, respectively. The C.E value (0.19) of the catalyst-coated RRDE was assessed using the reported procedure.[20]

We have performed steady-state chronoamperometry at E = 0.6 V in 0.1 M KOH solution saturated with oxygen. The results showed that around 80% of the initial current density was retained over a period of 25 h (Figure S9). This result suggests that the durability of the compound **1** as an ORR catalyst was superior compared to those of other MOF-based ORR catalysts and Pt nanoparticles (42%), Ni foam (48%), and so forth.[13,14]

A better ORR catalyst always maintains its structural and functional stability during electrochemical reactions. For the present case, we have carried out PXRD, microscopy techniques, IR spectroscopy, X-ray photoelectron spectroscopy (XPS) techniques, and inductively coupled plasma mass spectrometry (ICP-MS) to analyze the structural integrity after ORR activity (Figures S1a and S10–S13). PXRD data of compound **1** before and after the ORR experiment show that compound **1** maintained its structural integrity after ORR (Figure S1a). We have done stereomicroscopy and scanning electron microscopy (SEM) studies of the catalyst before and after ORR reactions (Figures S10 and S11). The overall morphology was unchanged upon electrochemical reactions under O_2. The SEM images after ORR appear to be rough, which might be the evidence of O_2 adsorption on the surface of the catalyst (Figure S11). The structural integrity was evidenced by IR spectroscopy carried out on the catalyst before and after electrochemical reactions (Figure S12). XPS studies of the catalyst before and after ORR revealed a slight shift in binding energy to a higher energy of the Co 2p region (780–790 eV) (Figure S13). This shift in binding energy could

DOI: 10.1021/acsomega.8b00088
ACS Omega 2018, 3, 3830–3834

be due to the interactions of the cobalt center with oxygen molecules. The ICP-MS result shows the negligible amount of cobalt in the electrolyte during electrochemical reactions under O_2 and hence rules out any possible destruction of the framework under oxygen reduction conditions (see the Supporting Information). All of these characterizations revealed that though the catalyst undergoes minor structural rearrangement during the electrochemical reaction under O_2, it retains the catalytic activity because the active sites were unaffected during electrocatalysis.

COMPUTATIONAL METHODS

We have carried out density functional theory calculations using M062X[21] functional to shed light on the oxygen-binding propensity of the monomeric and the trimeric units. For the ease of calculations, these units are modeled separately, keeping the same local environment around the Co centers; $Co(PhCO_2)_2Py_2$ is chosen as a model for the monomeric unit, whereas the trimeric unit is modeled with $Co_3(PhCO_2)_5(OH)Py_3$. Optimized structures of these units are given in the Supporting Information, and the computed structural parameters are consistent with the experimental data (Figure S14). The Kohn–Sham orbital analysis shows that lowest unoccupied molecular orbitals (LUMOs) in these model units are delocalized over the Co–Py fragments (Figure S15). The LUMO of the monomeric unit arises from the overlap between two π^* type antibonding orbitals of the Py ligands and a suitably oriented Co d-orbital. Such an overlap is favored by the linear disposition of the Py–Co–Py fragment (a N–Co–N bond angle 180°) in the monomer. The LUMO of the trimeric unit involves the Co(3) site which is attached to two Py ligands (CoO_4N_2 environment). However, in contrary to the monomer, the LUMO is delocalized over only one Co–Py fragment because of the nonlinearity of the N–Co–N fragment (a N–Co–N bond angle 96.1°). An inspection of the highest occupied molecular orbital (HOMO) of the oxygen molecule clearly indicates that O_2 coordination would occur in the monomeric unit owing to the favorable symmetric combination between the frontier orbitals (Figures 6 and S16). Such

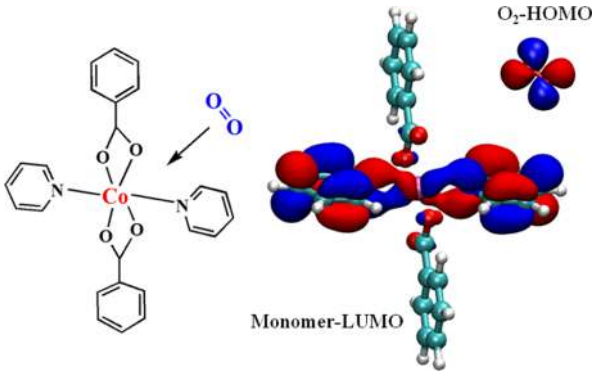

Figure 6. HOMO and LUMO positions of the monomer and schematic of interactions between monomer and O_2 molecule.

interactions are not viable at the Co(3) site of the trimer. In addition, in line with this observation, we have successfully located a complex of a monomer with O_2 coordinating at the Co site (side-on manner).[22] Complete ORR mechanism on this compound is being investigated in detail.

The mechanism and precise active sites of the M–N–C (Fe–N–C or Co–N–C) catalysts for ORR are still not very clear, which hinders the development and commercialization of these catalysts.[16] Recently, it was shown that unpyrolyzed MOFs can be used for ORR. The drawbacks of the unpyrolyzed MOFs are the low onset potential and incomplete reduction of oxygen, with less than $4e^-$ per oxygen molecule in 0.1 N KOH electrolyte. Mao et al. studied the (Cu-bipy-BTC) (bipy = 2,2′-bipyridine and BTC = 1,3,5-benzene tricarboxylic acid) MOF in a phosphate buffer electrolyte (pH = 6).[7] It shows oxygen reduction via a $4e^-$ pathway at 0.6 V versus RHE in a pH = 6 electrolyte. Miner et al. showed that Ni_3(hexaiminotriphenylene)$_2$ reduces oxygen via a $2e^-$ pathway in 0.1 N KOH.[12] Several Co- and Fe-based MOFs were used as templates in synthesizing electrocatalysts via pyrolysis method.[23−27] Although the catalysts synthesized from the pyrolysis method show higher ORR onset, the active sites involved in these pyrolyzed catalysts are not clearly known, thereby limiting the researchers' ability to engineer the catalysts to improve ORR. To design efficient ORR catalysts with precise information about the active sites, unpyrolyzed catalysts might be the better choice. Among the unpyrolyzed catalysts, the present compound **1** exhibits better ORR activity, which is comparable to other reported ORR activities (Table S3).

CONCLUSIONS

In summary, we have synthesized a new semiconductive three-dimensional cobalt-based CP, where trimeric and monomeric units are linked with the organic ligands to form the structural architecture. The electrical conductivity of compound **1** is 5×10^{-4} S cm^{-1}, and an optical band gap energy of 1.83 eV confirms its semiconductor nature. Interestingly, this compound shows oxygen reduction in alkali medium with a 3.6-electron-transfer process, leading to a near complete reduction of O_2 into OH^- ions. Methanol tolerance experiments revealed that this catalyst can act as a cathode material in DMFCs. Chronoamperometry studies showed that it can retain its current density up to 80% over a period of 25 h. This performance is much superior to those of any other reported MOFs or MOF–graphene composites in terms of durability. All state-of-the-art characterizations revealed that the present catalyst maintains its structural robustness during electrocatalysis. We have carried out theoretical calculations to understand the active catalytic center in the present catalyst, and they showed that O_2 molecules can effectively bind with the monomeric cobalt center. In addition, this is due to the efficient overlap of HOMO–LUMO between monomer and O_2 molecule. With this knowledge of the active catalytic site, presently we are working on synthesizing conducting inorganic–organic hybrid materials and unravel the mechanistic pathway for this electrocatalysis reaction.

ASSOCIATED CONTENT

Supporting Information

The Supporting Information is available free of charge on the ACS Publications website at DOI: 10.1021/acsomega.8b00088.

Detailed synthetic procedures, single-crystal X-ray diffraction data, PXRD, Fourier-transform infrared spectroscopy, TGA, SEM, stereomicroscopy images, XPS, solid-state absorption spectra, electrochemical data, theoretical calculations, and comparable ORR data with

DOI: 10.1021/acsomega.8b00088
ACS Omega 2018, 3, 3830−3834

reported catalysts and X-ray crystallography data for compound **1** (CCDC 1544167) (PDF)

AUTHOR INFORMATION

Corresponding Author

*E-mail: sukhendu@iisertvm.ac.in (S.M.).

ORCID

Swapan K. Pati: 0000-0002-5124-7455

Sukhendu Mandal: 0000-0002-4725-8418

Author Contributions

⊥A.S. and S.D. made equal contribution to this work.

Funding

Council of Scientific and Industrial Research (CSIR), Govt. of India, through a grant 01(2778)/14/EMR-II.

Notes

The authors declare no competing financial interest.

ACKNOWLEDGMENTS

We acknowledge Nagabhushan Hegde for his help during synthesis.

REFERENCES

(1) Bashyam, R.; Zelenay, P. A Class of Non-precious Metal Composite Catalysts for Fuel Cells. *Nature* **2006**, *443*, 63−66.

(2) Cheng, F.; Chen, J. Metal-air Batteries: from Oxygen Reduction Electrochemistry to Cathode Catalysts. *Chem. Soc. Rev.* **2012**, *41*, 2172−2192.

(3) Jaouen, F.; Herranz, J.; Lefèvre, M.; Dodelet, J.-P.; Kramm, U. I.; Herrmann, I.; Bogdanoff, P.; Maruyama, J.; Nagaoka, T.; Garsuch, A. Cross-laboratory Experimental Study of Non-noble-metal Electrocatalysts for Oxygen Reduction Reaction. *ACS Appl. Mater. Interfaces* **2009**, *1*, 1623−1639.

(4) Schafer, F. P.; et al. *Physical and Chemical Applications of Dyestuffs*; Springer, 1976.

(5) Chen, Z.; Higgins, D.; Yu, A.; Zhang, L.; Zhang, J. A Review on Non-precious Metal Electrocatalysts for PEM Fuel Cells. *Energy Environ. Sci.* **2011**, *4*, 3167−3192.

(6) Tang, H.; Yin, H.; Wang, J.; Yang, N.; Wang, D.; Tang, Z. Molecular Architecture of Cobalt Porphyrin Multilayers on Reduced Graphene Oxide Sheets for High-performance Oxygen Reduction Reaction. *Angew. Chem., Int. Ed.* **2013**, *52*, 5585−5589.

(7) (a) Mao, J.; Yang, L.; Yu, P.; Wei, X.; Mao, L. Electrocatalytic Four-electron Reduction of Oxygen with Cu(II)-based Metal-Organic Framework. *Electrochem. Commun.* **2012**, *19*, 29−31. (b) Li, J.-S.; Li, S.-L.; Tang, Y.-J.; Li, K.; Zhou, L.; Kong, N.; Lan, Y.-Q.; Bao, J.-C.; Dai, Z.-H. Heteroatoms ternary-doped porous carbons derived from MOFs as metal-free electrocatalysts for oxygen reduction reaction. *Sci. Rep.* **2014**, *4*, 5130.

(8) (a) Jiang, M.; Li, L.; Zhu, D.; Zhang, H.; Zhao, X. Oxygen Reduction in the Nanocage of Metal-Organic Framework with an Electron transfer Mediator. *J. Mater. Chem. A* **2014**, *2*, 5323−5329. (b) Li, J.-S.; Li, S.-L.; Tang, Y.-J.; Han, M.; Dai, Z.-H.; Bao, J.-C.; Lan, Y.-Q. Nitrogen-doped Fe/Fe3C@graphitic layer/carbon nanotube hybrids derived from MOFs: efficient bifunctional electrocatalysts for ORR and OER. *Chem. Commun.* **2015**, *51*, 2710−2713.

(9) (a) Wang, H.; Yin, F.; Chen, B.; Li, G. Synthesis of an ε-MnO_2/Metal-Organic Framework Composite and its Electrocatalysis Towards Oxygen Reduction Reaction in Alkaline Electrolyte. *J. Mater. Chem. A* **2015**, *3*, 16168−16176. (b) Li, J.; Chen, Y.; Tang, Y.; Li, S.; Dong, H.; Li, K.; Han, M.; Lan, Y.-Q.; Bao, J.; Dai, Z. Metal-organic Framework Templated Nitrogen and Sulfur co-doped Porous Carbons as Highly Efficient Metal-free Electrocatalysts for Oxygen Reduction Reactions. *J. Mater. Chem. A* **2014**, *2*, 6316−6319.

(10) Sun, L.; Campbell, M. G.; Dincă, M. Electrically Conductive Porous Metal-Organic Frameworks. *Angew. Chem., Int. Ed.* **2016**, *55*, 3566−3579.

(11) Zhang, P.; Hou, X.; Liu, L.; Mi, J.; Dong, M. Two-dimensional π-Conjugated Metal Bis(dithiolene) Complex Nanosheets as Selective Catalysts for Oxygen Reduction Reaction. *J. Phys. Chem. C* **2015**, *119*, 28028−28037.

(12) Miner, E. M.; Fukushima, T.; Sheberla, D.; Sun, L.; Surendranath, Y.; Dincă, M. Electrochemical Oxygen Reduction Catalysed by Ni_3(hexaminotriphenylene)$_2$. *Nat. Commun.* **2016**, *7*, 10942.

(13) Jahan, M.; Bao, Q.; Loh, K. P. Electrocatalytically Active Graphene-porphyrin MOF Composite for Oxygen Reduction Reaction. *J. Am. Chem. Soc.* **2012**, *134*, 6707−6713.

(14) Aijaz, A.; Fujiwara, N.; Xu, Q. From Metal-Organic Framework to Nitrogen-Decorated Nanoporous Carbons: High CO_2 Uptake Efficient Catalytic Oxygen Reduction. *J. Am. Chem. Soc.* **2014**, *136*, 6790−6793.

(15) Shen, K.; Chen, X.; Chen, J.; Li, Y. Development of MOF-Derived carbon-Based Nanomaterials for Efficient Catalysis. *ACS Catal.* **2016**, *6*, 5887−5903.

(16) Zhao, S.; Yin, H.; Du, L.; He, L.; Zhao, K.; Chang, L.; Yin, G.; Zhao, H.; Liu, S.; Tang, Z. Carbonized Nanoscale Metal-Organic Frameworks as High performance Electrocatalyst for Oxygen Reduction reaction. *ACS Nano* **2014**, *8*, 12660−12668.

(17) Shao, M.; Chang, Q.; Dodelet, J.-P.; Chenitz, R. Recent Advances in Electrocatalysts for Oxygen Reduction Reaction. *Chem. Rev.* **2016**, *116*, 3594−3657.

(18) Zhang, E.; Xie, Y.; Ci, S.; Jia, J.; Cai, P.; Yi, L.; Wen, Z. Multifunctional High-activity and Robust Electrocatalyst Derived from Metal-Organic Frameworks. *J. Mater. Chem. A* **2016**, *4*, 17288−17298.

(19) Blatov, V. A.; Proserpio, D. M. Topological Relations between Three-Periodic Nets. II. Binodal Nets. *Acta Crystallogr., Sect. A: Found. Crystallogr.* **2009**, *65*, 202−212.

(20) Paulus, U. A.; Schmidt, T. J.; Gasteiger, H. A.; Behm, R. J. Oxygen Reduction on a High Surface Area Pt/Vulcan carbon catalyst: A Thin-film Rotating Ring-disk Electrode Study. *J. Electroanal. Chem.* **2001**, *495*, 134−145.

(21) Zhao, Y.; Truhlar, D. G. A New Local Density Functional for Main-group Thermochemistry, Transition Metal Bonding, Thermochemical Kinetics, and Noncovalent Interactions. *J. Chem. Phys.* **2006**, *125*, 194101.

(22) However, attempts to computationally optimize a complex with the coordination of O_2 at the site Co(3) of trimer led to separated species such as O_2 and trimer. This can as well be due to the steric congestion at the Co(3) site preventing the coordination of O_2.

(23) Han, J.; Sa, Y. J.; Shim, Y.; Choi, M.; Park, N.; Joo, S. H.; Park, S. Coordination Chemistry of [Co(acac)$_2$] with N-doped Graphene: Implications for Oxygen Reduction Reaction Reactivity of Organometallic Co-O4-N Species. *Angew. Chem., Int. Ed.* **2015**, *54*, 12622−12626.

(24) Xi, J.; Xia, Y.; Xu, Y.; Xiao, J.; Wang, S. (Fe, Co) @ Nitrogen-doped Graphitic Carbon Nanocubes Derived from Polydopamine-encapsulated Metal-Organic Frameworks as a Highly Stable and Selective-Non-precious Oxygen Reduction Electrocatalyst. *Chem. Commun.* **2015**, *51*, 10479−10482.

(25) Bezerra, C. W. B.; Zhang, L.; Lee, K.; Liu, H.; Marques, A. L. B.; Marques, E. P.; Wang, H.; Zhang, J. A Review of Fe-N/C and Co-N/C Catalysts for the Oxygen reduction reaction. *Electrochim. Acta* **2008**, *53*, 4937−4951.

(26) Long, J.; Li, R.; Gou, X. Well-organized Co-Ni@NC Material Derived from Heterodinuclear MOFs as Efficient Electrocatalysts for Oxygen Reduction. *Catal. Commun.* **2017**, *95*, 31−35.

(27) Li, X.; Jiang, Q.; Dou, S.; Deng, L.; Huo, J.; Wang, S. ZIF-67 Derived Co-NC@Co-P-NC Nanopolyhedra as an Efficient Bifunctional Oxygen Electrocatalyst. *J. Mater. Chem. A* **2016**, *4*, 15836−15840.

DOI: 10.1021/acsomega.8b00088
ACS Omega 2018, 3, 3830−3834